JACS
JOURNAL OF THE AMERICAN CHEMICAL SOCIETY
Article
Cite This: J. Am. Chem. Soc. 2018, 140, 2546−2554
pubs.acs.org/JACS

Modular Approach to Kekulé Diradicaloids Derived from Cyclic (Alkyl)(amino)carbenes

Max M. Hansmann, Mohand Melaimi, Dominik Munz, and Guy Bertrand*

UCSD-CNRS Joint Research Laboratory (UMI 3555), Department of Chemistry and Biochemistry, University of California San Diego, La Jolla, San Diego, California 92093-0358, United States

Supporting Information

ABSTRACT: A modular approach for the synthesis of Kekulé diradicaloids is reported. The key step is the insertion of a carbene, namely, a cyclic (alkyl)(amino)carbene (CAAC), into the C−H bonds of two terminal alkynes linked by a spacer. Subsequent hydride abstraction, followed by two-electron reduction of the corresponding bis(iminium) salts, affords the desired diradicaloids. This synthetic route readily allows for the installation of communicating spacers, featuring different degrees of aromaticity and lengths, and gives the possibility of generating unsymmetrical compounds with two different CAACs. Electron paramagnetic resonance (EPR), NMR, UV−vis, and X-ray studies in combination with quantum-chemical calculations give insight into the electronic nature of the deeply colored Kekulé diradicaloids. They feature a singlet ground state with varying degrees of diradical character in combination with small singlet/triplet gaps. Upon lengthening of the spacer, the properties of the compounds approach those of monoradicals in which steric protection of the propargyl radical moiety is necessary to inhibit decomposition pathways. Most of these diradicaloids are stable at room temperature, both in solution and in the solid state, but are highly oxygen-sensitive. They represent the first diradicaloids derived from iminium salts.

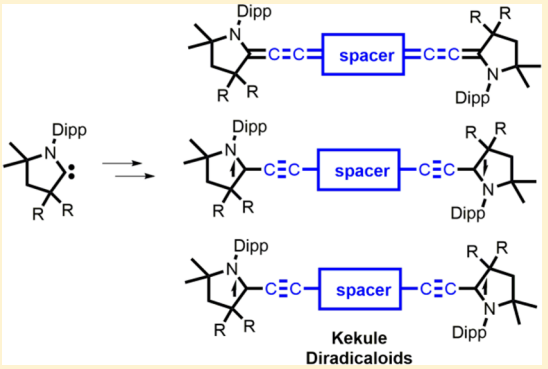

INTRODUCTION

Organic molecules with two unpaired electrons (either singlet or triplet) are of fundamental importance in understanding the nature of chemical bonding.[1] Shortly after Gomberg's discovery of the triphenylmethyl radical in 1900,[2] Tschitschibabin synthesized the first stable organic diradical **I**[3] (Figure 1).

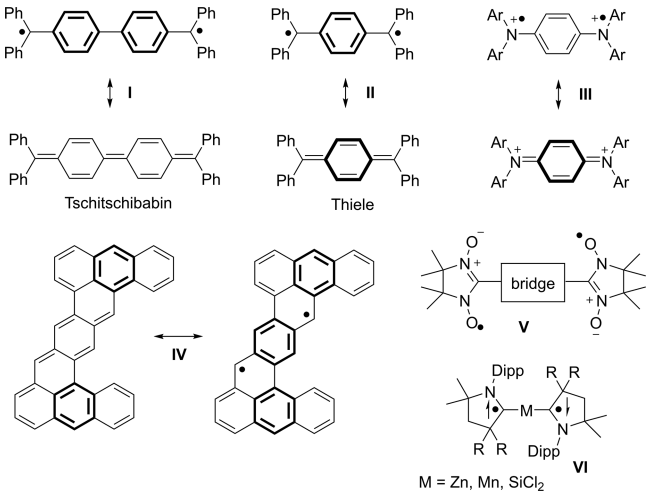

Figure 1. Selection of typical representatives of organic Kekulé diradicals and related molecules.

Since then this molecule has triggered a very controversial discussion about organic diradicals/diradicaloids and the nature of the "diradical paradox".[4] Indeed, **I** can be described as either a diradical or a cumulene structure in which the loss of aromaticity is compensated by spin-pairing (Clar's sextet rule).[5] Nowadays, it is generally believed that Tschitschibabin hydrocarbon **I** has to be considered as a diradicaloid.[6] In contrast, Thiele's hydrocarbon **II**[7] and triarylamine dications **III**,[8] which contain only one benzene spacer between the two radical centers, are best described as cumulenes. Many other extended *p*-quinodimethanes (Kekulé diradicals), such as zethrenes **IV**, which can also be regarded as graphene nanoflakes,[9] feature open-/closed-shell behavior. Note also that a few singlet and triplet diradicals of main group elements have been reported,[10] as well as studies on the through-space spin−spin interaction between stable free radicals derived from nitroxides (**V**).[11] Molecules with switchable electronic states not only are of fundamental interest but also show unique applications in material science, ranging from nonlinear optics to spintronics, photovoltaics, and energy-storage devices.[12] Recently, our group and others have demonstrated that cyclic (alkyl)(amino)carbenes (CAACs)[13,14] are excellent ligands for stabilizing a variety of paramagnetic organic,[15] main group, and transition metal species.[16,17] Interestingly, when two CAACs

Received: October 26, 2017
Published: January 31, 2018

DOI: 10.1021/jacs.7b11183
J. Am. Chem. Soc. 2018, 140, 2546−2554

are coordinated to either Zn, Mn,[18] or $SiCl_2$,[19] it has been demonstrated that such systems can be described as diradicaloids in which two antiferromagnetic coupled radicals reside on the CAAC moiety (**VI**).

CAACs have also been used to prepare compound **VII**.[20] This species was regarded as a biscarbene-stabilized C_2[21] (**VIIa**) and as a cumulene (**VIIb**). Because the spacer between the two CAACs is short, the energy required for unpairing the two electrons is very high, and thus it is clear that this compound cannot be a singlet diradical (**VIIc**). By analogy with Thiele/Tschitschibabin hydrocarbons, we wondered if an aromatic-containing spacer would allow for the preparation of diradicals based on CAACs, and here we report our findings.

RESULTS AND DISCUSSION

To access a broad range of these species, we aimed for a modular approach in which the carbene and spacer components could easily be tuned. We and others have shown that C−H activation of alkynes with carbenes, especially CAACs **1**, is highly selective.[15e,22] Therefore, we considered a double C−H activation of a diyne spacer **2**, giving **3**, followed by two hydride abstractions affording **4** (Scheme 1), which by

Scheme 1. Synthesis of Symmetrical (a) and Unsymmetrical (b) Bis(iminium) Salts 4a

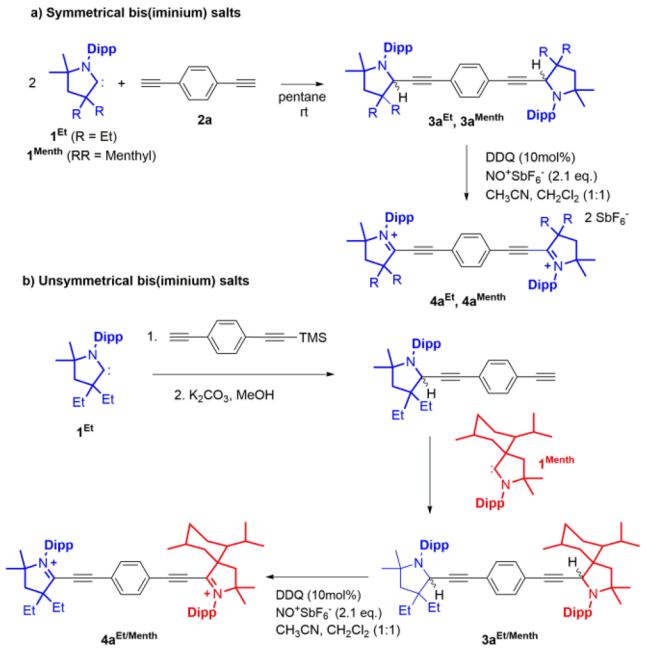

subsequent two-electron reduction of the bisiminium salts would afford the desired diradicaloids. We started our investigation by reacting the diethyl-CAAC ($\mathbf{1}^{Et}$) and menthyl-CAAC ($\mathbf{1}^{Menth}$) with 1,4-diethynylbenzene (**2a**), which cleanly gave diastereomeric mixtures of the bis-C−H activation products $\mathbf{3a}^{Et}$ and $\mathbf{3a}^{Menth}$, respectively. Then, we tested several conditions to abstract the two hydrides to transform **3** into the bisiminium salts **4**. While trityl and Br^+ sources proved to be unselective, the use of 2.5 equiv of 2,3-dichloro-5,6-dicyano-1,4-benzoquinone (DDQ) was efficient to abstract the hydrides, but the reduced DDQ is (i) difficult to exchange by salt metathesis and (ii) slowly adds to the highly electrophilic bisiminium salts (see section S2 in the Supporting Information for an X-ray analysis of such a byproduct). These hurdles were overcome by using a redox system in which DDQ was employed catalytically (10 mol %) and regenerated with $NOSbF_6$ (2.1 equiv). This novel synthetic route turned out to be very general and was used throughout this study for the synthesis of bisiminium salts containing SbF_6^- as counteranion. This modular approach can be extended to unsymmetrical compounds as shown by $\mathbf{4a}^{Et/Menth}$. Indeed, the reaction of CAAC $\mathbf{1}^{Et}$ with mono-trimethylsilyl (TMS)-protected 1,4-dialkynylbenzene afforded cleanly the C−H activation product. After deprotection, the compound was reacted with a second carbene ($\mathbf{1}^{Menth}$) to afford $\mathbf{3a}^{Et/Menth}$ as a mixture of diastereomers. Subsequent hydride abstraction under the established conditions led to $\mathbf{4a}^{Et/Menth}$ in excellent yield. Interestingly, the two ^{13}C iminium resonances of $\mathbf{4a}^{Et/Menth}$ are well-separated at 179.9 and 177.9 ppm and match with the values from the $\mathbf{4a}^{Et}$ (179.8 ppm) and $\mathbf{4a}^{Menth}$ (177.9 ppm) derivatives.

The cyclic voltammograms of $\mathbf{4a}^{Et}$, $\mathbf{4a}^{Menth}$, and $\mathbf{4a}^{Et/Menth}$ show two quasireversible reduction waves centered around $E_{1/2}$ = −0.72 and −0.98 V (versus Fc^+/Fc) with a splitting of about ΔE = 270 mV (Figure 2). In agreement with the reduction

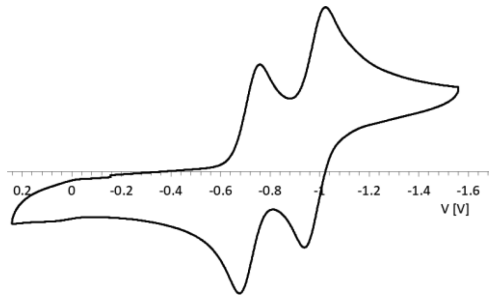

Figure 2. Cyclovoltamogram of $\mathbf{4a}^{Et}$ (nBu$_4$NPF$_6$ 0.1 M in tetrahydrofuran (THF), 100 mV s^{-1}, vs Fc^+/Fc).

potentials, the addition of 2 equiv of cobaltocene to salts **4a** resulted in intense purple-colored solutions of $\mathbf{5a}^{Et}$, $\mathbf{5a}^{Menth}$, and $\mathbf{5a}^{Et/Menth}$. All these compounds are stable in solution and in the solid state over several days but are very sensitive toward oxygen. As shown in Scheme 2, using $\mathbf{5a}^{Et}$ as an illustration,

Scheme 2. Reduction of Bis(iminium) Salt $\mathbf{4a}^{Et}$ and Schematic Representations of the Different Possible Electronic States of $\mathbf{5a}^{Et}$

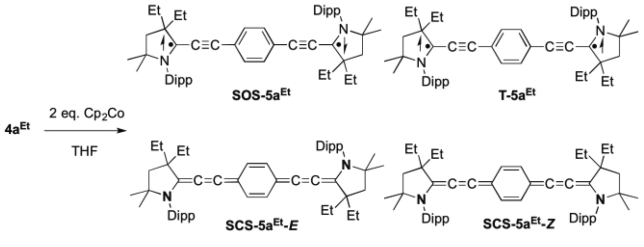

three electronic states should be considered: singlet open shell (**SOS**), triplet (**T**), and singlet closed shell (**SCS**) or cumulene as Z and E isomers.[23]

The unusually intense purple color of solutions of **5a** and the metallic luster of the corresponding crystals, along with the high sensitivity toward oxygen, already indicate that the electronic structure of derivatives **5a** is more complex than a simple diamagnetic cumulene. At room temperature, only very broad

DOI: 10.1021/jacs.7b11183
J. Am. Chem. Soc. 2018, 140, 2546−2554

signals corresponding to the CAAC fragments were oberved in the ^{1}H NMR spectra of compounds **5a**, while the ^{13}C NMR spectra were silent. This could mean either that these compounds exhibit a paramagnetic ground state, that they exhibit a thermally populated paramagnetic excited state, or that the solutions contain a paramagnetic impurity. However, upon cooling a toluene-d_8 solution of **5a**^{Et}, new ^{1}H NMR resonances appeared in the alkene region (Figure 3). At −50 °C two sets of

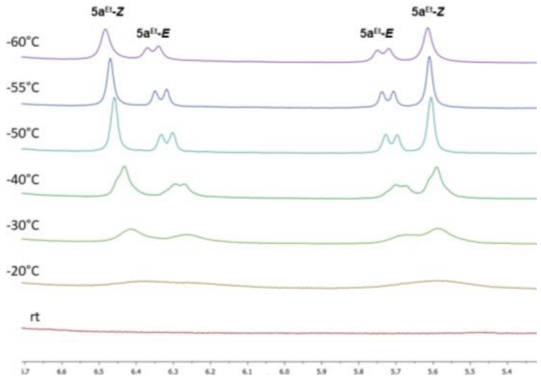

Figure 3. Selected region of the temperature-dependent NMR spectra of **5a**^{Et} in toluene-d^8.

signals at δ = 6.46 (s) and 5.60 (s) ppm, and δ = 6.30 (d, J = 9.3 Hz) and 5.70 (d, J = 9.3 Hz) ppm, were clearly observed. These signals are those expected for the Z and E isomers (1:0.6 mixture) of quinoid structures (**SCS-5a**^{Et}).[24] This observation suggests that **5a** has a singlet ground state with a paramagnetic excited state that is populated at room temperature. Note that variable-temperature (VT) NMR experiments have been used in the literature for the detection of open-shell singlet ground states as the broad resonances of singlet diradical species become sharper at lower temperatures.[8,25]

EPR measurements were carried out to observe **5a** in their triplet state. The EPR spectrum of **5a**^{Et} in pentane at room temperature shows only coupling to one nitrogen and can be fitted with a_N = 5.6 G (Figure 4). To rule out that an impurity was reponsible for the EPR signal, we measured the EPR spectrum of **5a**^{Menth}. The latter could be fitted with a_N = 5.5 G and a_H = 2.2 G, while for **5a**$^{Et/Menth}$, a combination of the two signals of **5a**^{Et} and **5a**^{Menth} (a_N = 5.5 and 5.8 G and a_H = 2.9 G) was observed. The additional proton coupling in the case of

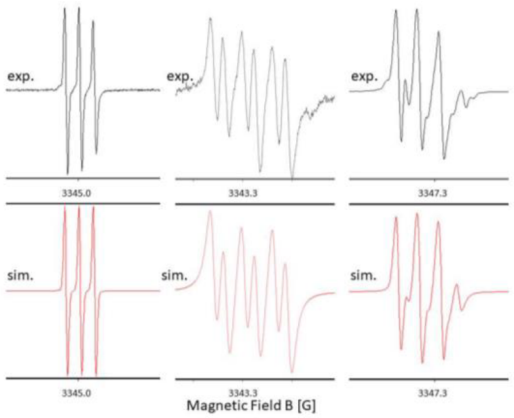

Figure 4. EPR spectra of **5a**^{Et} (left), **5a**^{Menth} (middle), and **5a**$^{Et/Menth}$ (right) at room temperature in pentane.

5a^{Menth} can be explained by the recently described coupling with one H of the menthyl backbone.[22c] As the EPR signal of a weakly populated triplet state is very sensitive to a paramagnetic impurity containing an open-shell ground state, the analysis of EPR spectra should be taken with caution. Note that the EPR spectra of molecules such as Tschitschibabin hydrocarbon **I** have been subject to very controversial EPR discussions without a clear answer.[4] On the basis of the EPR spectra of **5a**^{Et}, **5a**^{Menth}, and **5a**$^{Et/Menth}$, it seems likely that in the triplet state the radicals are centered onto the outer CAAC ligands with small contribution of the spacer element. Indeed, CASSCF(10,10) calculations (vide infra) show that in the triplet state the spin densities in **5a** are centered onto the CAAC moieties without significant contribution from the phenyl spacer (see Figure S23). X-band EPR measurements performed in the solid state resulted in a very broad unresolved resonance (g = 3364 G); however, at elevated temperatures (325 K) we could detect the corresponding half-field signal (g = 1682 G), demonstrating the triplet diradical nature of **5a** (Figure 5). In agreement with the NMR data, we observed a decrease of the EPR signal intensity upon cooling, but we were not able to fit the data to obtain the singlet−triplet gap.

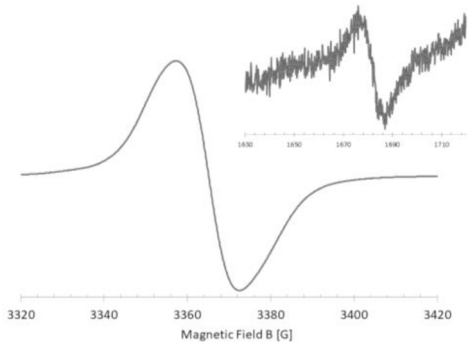

Figure 5. Solid-state X-band EPR spectrum of **5a**^{Menth} at 325 K with inset showing the half-field signal.

Attempts to measure the magnetic properties of **5a**^{Et} by SQUID only resulted in the detection of a small amount of temperature-independent paramagnetism and did not show any significant magnetism up to 350 K (see section S6, Supporting Information). This observation is in agreement with a singlet ground state (open or closed) and a triplet state being at least 4−5 kcal/mol above the ground state.

We were able to obtain deep purple single crystals of **5a**^{Et} and **5a**^{Menth} at −40 °C, and X-ray crystallographic analyses were carried out at 100 K (Figure 6). When comparing the geometric parameters of **5a**^{Et} with those of its dicationic precursor **4a**^{Et} (Table 1), it appears that there is a lengthening of the C2−C3 "triple" bond [1.236(3) Å] and a shortening of the C1−C2 [1.343(4) Å] and C3−C4 [1.363(3) Å] "single" bonds. Note that the two nitrogen atoms are located in a nearly perfect trans-fashion, indicating no free rotation around the C1−C2 axis at 100 K.

To obtain more insight into the electronic structure of **5a**, we performed density functional theory (DFT) calculations. We optimized the structure of **5a**^{Et} using R/(U)B3LYP, R/(U)CAM-B3LYP, and R/(U)M05-2X functionals, which have been popular choices in the literature for diradicals,[26] in combination with 6-31G**/TZVP basis sets for the three SOS, SCS, and triplet states (Table 1; see also Supporting

DOI: 10.1021/jacs.7b11183
J. Am. Chem. Soc. 2018, 140, 2546−2554

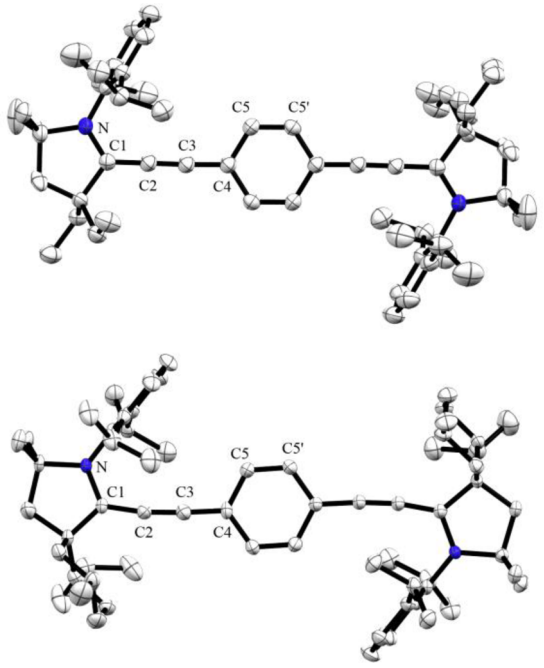

Figure 6. Solid-state molecular structures of $\mathbf{5a}^{Et}$ (top) and $\mathbf{5a}^{Menth}$ (bottom). Hydrogen atoms are omitted for clarity. Selected bond parameters for $\mathbf{5a}^{Menth}$ in (Å) and (deg) as averaged for left and right sides of the molecule: N−C1 1.380(5), C1−C2 1.362(6), C2−C3 1.245(6), C3−C4 1.375(5), C4−C5 1.437(5), C5−C5′ 1.362(5), N−C1−C2 120.4(3), C1−C2−C3 171.0(4), C2−C3−C4 173.6(4), and N−C1−C1′-N′ 4.9(3) (for $\mathbf{5a}^{Et}$, see Table 1).

Information). To analyze the singlet open-shell state, the broken-symmetry (BS) formalism proposed by Noodleman and Yamaguchi was chosen.[27] Comparing the calculated and experimental geometric parameters for $\mathbf{5a}^{Et}$, it seems quite likely that at 100 K this compound is best described as a singlet (open- or closed-shell) species. This conclusion is also in good agreement with the variable-temperature NMR and EPR data. Note that, in the hope of observing **5a** with a partially populated triplet state, we carried out X-ray analyses at 100 and 270 K, but the variation of the geometric parameters cannot be easily rationalized. (The crystal structure of Tschitschibabin hydrocarbon recorded at three different temperatures did not show any significant change in bond distances either.[6a])

We also noticed that the choice of the functional can have a significant impact on the relative energy of the three electronic states. In agreement with the experimental data, all functionals investigated predict a singlet ground state (either closed or open shell) and a higher-lying triplet state. Both the BS-UCAM-B3LYP/6-31G** and BS-UM05-2X/6-31G** calculations predict an open-shell singlet ground state (SOS), which is 1.3−3.8 and 7.5−8.4 kcal/mol lower in energy than the SCS state and triplet state, respectively [note that, at the B3LYP/TZVP (or 6-31G**) level, a cumulene ground state (SCS) is predicted] (see Supporting Information). According to Yamaguchi et al.,[27] as the BS method admixes the singlet with the triplet state, a spin-correction (SC) is necessary to obtain more accurate S/T energy gaps. The spin-contamination can be determined from the calculated values of the spin-operators $\langle S^2 \rangle$. While for a triplet state $\langle S^2 \rangle$ should be 2, the value for a pure singlet diradical state in the BS method should be 1. Using UCAM-B3LYP/6-31G** and UM05-2X/6-31G**, the calculated $\langle S^2 \rangle_{BS}$ values for $\mathbf{5a}^{Et}$ are 0.86 and 0.66, which leads to $\Delta_{SOS/T}{}^{SC}$ values of 12.9 and 12.5 kcal/mol, respectively (see Supporting Information). Because the $\langle S^2 \rangle$ value is significantly larger than zero and in a typical range for semiquinoide diradical values (0.7−0.8),[4] it seems likely that $\mathbf{5a}^{Et}$ possesses a SOS-diradical ground state with a relatively large singlet−triplet gap. Note that the classical Tschitschibabin hydrocarbon diradical (**I**) exhibits a singlet−triplet energy gap of 8.1 kcal/mol with a $\langle S^2 \rangle$ of 0.77 at the BS-B3LYP/6-31G* level.[4] Furthermore, because the description of singlet biradicals is a challenge for single-reference methods like DFT, we performed multireference CASSCF calculations with a (10,10) active space including second-order correction for dynamic correlation effects (NEVPT2). Inded, a singlet ground state with considerable biradical character, i.e., population of the antibonding lowest unoccupied molecular orbital (LUMO) by 0.3 electrons (biradical index of 0.3), and a singlet−triplet gap of 15.2 kcal/mol were obtained for $\mathbf{5a}^{Et}$ (see Supporting Information). Thus, all computational methods suggest that **5a** can be classified as a singlet biradicaloid.

To investigate further the communication between the CAAC radical centers, bis(iminium) $\mathbf{4b}^{Menth}$ and $\mathbf{4c}^{Menth}$ (Scheme 3), featuring two Kekulé spacers with different degrees of aromaticity and lengths, were prepared using the modular approach described in Scheme 1 (see Supporting Information).

Table 1. Experimental and Calculated Bond Distances (a) from X-ray Diffraction at 100 K and (b) Calculated at the (U)/RCAM-B3LYP/6-31G (top) and (U)/RM05-2X/6-31G** Levels (bottom), Respectively**

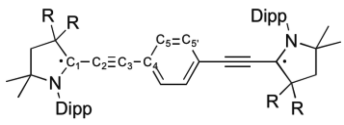

		$N-C_1$	C_1-C_2	C_2-C_3	C_3-C_4	C_4-C_5	$C_5-C_{5'}$
$\mathbf{4a}^{Et}$	exp. (a)	1.289(4)	1.411(4)	1.186(4)	1.428(4)	1.390(5)	1.377(4)
$\mathbf{5a}^{Et}$	exp. (a)	1.367(3)	1.343(4)	1.236(3)	1.363(3)	1.440(4)	1.346(3)
	SCS (b)	1.376	1.336	1.255	1.346	1.452	1.348
		1.369	1.341	1.256	1.349	1.453	1.350
	SOS (b)	1.380	1.355	1.240	1.384	1.426	1.367
		1.372	1.353	1.245	1.376	1.433	1.364
	triplet (b)	1.384	1.374	1.227	1.419	1.406	1.382
		1.377	1.376	1.229	1.418	1.409	1.383

DOI: 10.1021/jacs.7b11183
J. Am. Chem. Soc. 2018, 140, 2546−2554

Scheme 3. Different Spacers Investigated with the Distance (r) between the Two Carbene Carbons

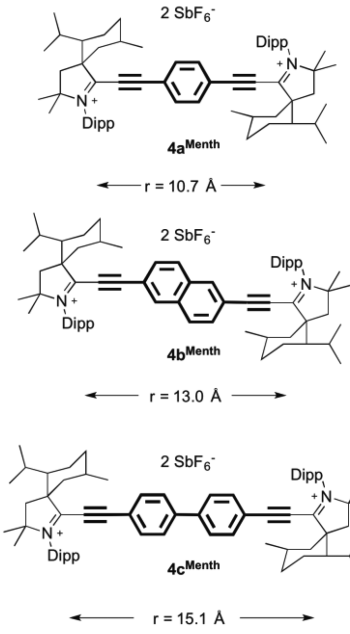

According to cyclic voltammetry studies, increasing the spacer length significantly shifts the first reduction potential from $E_{1/2}$ = −0.72 V (**4a**^{Menth}) to −0.82 V (**4b**^{Menth}) and −0.99 V (**4c**^{Menth}) but has little influence on the shift of the second reduction potential from $E_{1/2}$ = −0.98 V (**4a**^{Menth}) to −1.03 V (**4b**^{Menth}) and −1.08 V (**4c**^{Menth}). This is a first indication that longer spacers weaken the communication between the two radical centers. The two-electron reduction of bisiminium **4b**^{Menth} and **4c**^{Menth} with 2 equiv of cobaltocene proceeded cleanly at room temperature, affording **5b**^{Menth} and **5c**^{Menth}, respectively (Scheme 4). All compounds are deeply colored, very sensitive toward oxygen, but indefinitely storable under inert atmosphere in the solid state and in solution. Room-temperature UV−vis spectra of a pentane solution of **5a**^{Menth} feature two intense absorption bands at λ_{max} = 545 and 571 nm (log ε = 4.78 M^{-1} cm^{-1}, Figure 7). In line with the VT-NMR

Scheme 4. Synthesis of Neutral Diradicaloids 5b^{Menth} **and 5c**^{Menth} **with Their Schematic Representations of Diradical and SCS Electronic States**

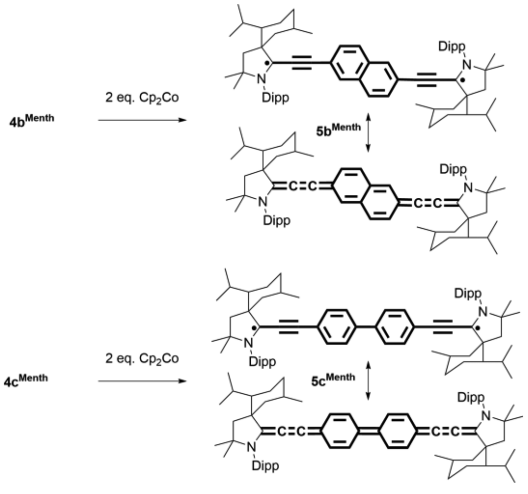

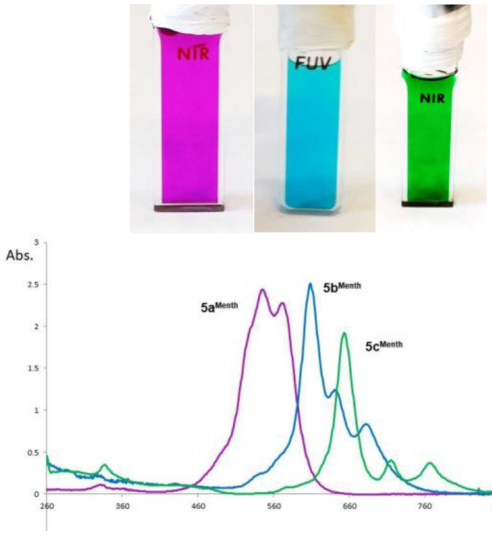

Figure 7. UV−vis spectra of **5a−c**^{Menth} in pentane solution and their optical appearance (top).

conclusions, time-dependent (TD)-DFT calculations (M06-2X/6-31G**) predict that the two bands arise from the presence of both the E and Z isomers. CASSCF(10,10) calculations reveal that these bands can be assigned to the closed-shell singlet to open-shell singlet transition. Interestingly, temperature-dependent UV−vis measurements show that the isomeric ratio Z/E increases upon cooling, in agreement with the TD-DFT and VT-NMR results (see Figures S18 and S19). UV−vis spectra of **5b**^{Menth} and **5c**^{Menth} were also recorded [**5b**^{Menth}: λ_{max} = 608, 641, and 682 nm, log ε = 5.10−4.62 M^{-1} cm^{-1}; **5c**^{Menth}: λ_{max} = 653, 717, and 767 nm, log ε = 4.72−4.21 M^{-1} cm^{-1}] (Figures 7 and S20). In the case of **5c**^{Menth}, TD-DFT reaches its limits and cannot accurately predict the observed transitions. However, preliminary CASSCF(8,8) calculations suggest SCS → SOS transitions with wavelengths of 601 nm (E-isomer) and 644 nm (Z-isomer).

Similar to that for **5a**^{Et}, the room-temperature ^{1}H NMR spectrum of **5b**^{Menth} shows only very broad signals. However, sharp signals characteristic for a mixture of E/Z quinoid structures appear upon cooling to −60 °C (see Supporting Information). In contrast, no ^{1}H NMR signals could be observed for **5c**^{Menth} even upon cooling to −70 °C.

We also prepared the green monomeric radical **6**^{Menth} by reduction of the corresponding iminium salt (see Supporting Information). Interestingly, the EPR obtained for this model system [**6**^{Menth}; a_N = 4.20 G, a_{Ha} = 2.75 G, a_{Hc} = 2.36 G, and a_{Hb} = 0.72 G] fits very well with the spectrum of **5c**^{Menth} [a_N = 4.04 G, a_{Ha} = 2.86 G, a_{Hc} = 2.17 G, and a_{Hb} = 0.67 G], indicating that in the triplet state the two radical centers of **5c**^{Menth} only weakly interact (Figure 8). X-band EPR solid-state measurements of **5c**^{Menth} shows a broad unresolved signal, in addition to the characteristic half-field resonance as expected for a triplet state (Figure 8). Furthermore, **6**^{Menth} shows a UV−vis absorption at 645 nm in THF, very similar to the main absorption of **5c**^{Menth} (653 nm).

Further proof for the presence of two weakly coupled radicals in **5c**^{Menth} was given by comparing its stability with that of **5c**^{Et}, featuring the smaller diethyl-CAAC ligand. At −78 °C, the addition of 2 equiv of cobaltocene to bis(iminium) **4c**^{Et} afforded the same green-colored solution as **5c**^{Menth}, which indicates the generation of **5c**^{Et} (Scheme 5). However, in

DOI: 10.1021/jacs.7b11183
J. Am. Chem. Soc. 2018, 140, 2546−2554

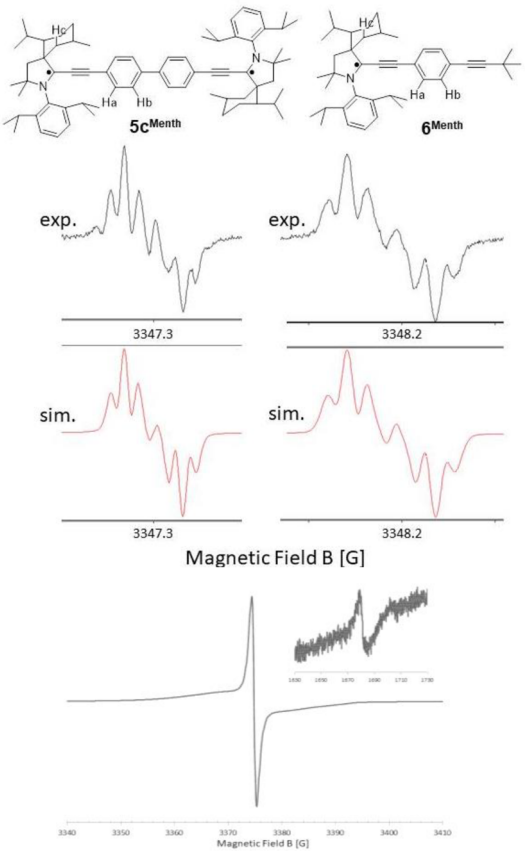

Figure 8. Comparison of the EPR spectra of **5c**^{Menth} and monomeric radical **6**^{Menth}; solid-state X-band EPR of **5c**^{Menth} (325 K) with inset showing the half-field signal.

Scheme 5. (a) Instability of Diradical 5c^{Et}**; (b) Reported Dimerization of Monoradical 8**^{Et}

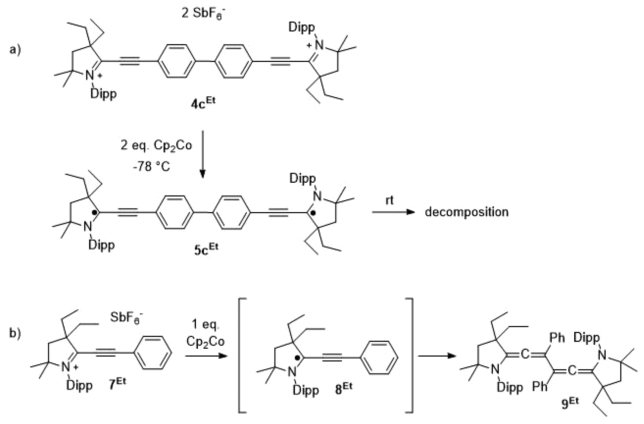

contrast to **5c**^{Menth}, upon warming to room temperature, **5c**^{Et} decomposed. The instability of **5c**^{Et} compared with the stability of **5a**^{Et} gives a good indication that **5c** contains more weakly coupled radical centers, thereby reacting similarly to a monoradical. Note that we have already reported that the monomeric radical **8**^{Menth} is stable in solution while the sterically unprotected radical **8**^{Et} dimerizes through the alkyne moiety, giving **9**^{Et} (Scheme 5b).[22c]

Deep green single crystals of **5c**^{Menth} were grown at −40 °C and subjected to an X-ray diffraction study (Figure 9). Most strikingly, as observed for Tschitschibabin hydrocarbon,[6a] the

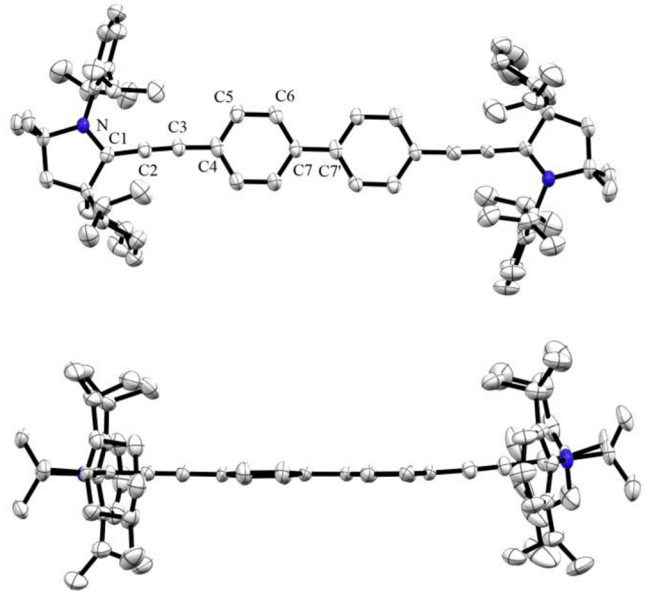

Figure 9. X-ray solid-state structure of **5c**^{Menth}; view from top and side. Hydrogen atoms are omitted for clarity, and only one molecule in the unit cell is shown (*E* isomer).

two phenyl groups are coplanar (dihedral angle ca. 2−3°). As in **5a**^{Et} and **5a**^{Menth}, the two nitrogens of **5c**^{Menth} are in a perfect *E* and *Z* geometry (both the *Z* and *E* isomers are independent molecules in the unit cell; see Supporting Information and Table 2), indicating some partial cumulene character. Some key bond distances on the central biphenyl moiety should be noted (for a more comprehensive comparison, see Supporting Information). The central C−C bond (1.439−1.442 Å) is significantly longer than a typical double bond, only slightly shorter than the single bond in biphenyl [X-ray, 1.493(3) Å;[28] neutron diffraction 1.495 Å[29]], and strikingly similar to known biradicals such as the central C−C distance of the Tschitschibabin hydrocarbon [1.448(4)][6a] and of extended viologen [1.438(3)].[30] Note that we did not observe significant differences in bond distances when measurements were done at 100 and 200 K.

DFT calculations were performed in order to compare the geometric parameters and electronics of the three diradicaloids **5a−c**. The (U)CAM-B3LYP/6-31G** and (U)M05-2X/6-31G** calculations gave comparable results (Table 2). The coplanarity of the phenyl rings, observed by X-ray crystallography, is only reproduced in the calculated SCS. However, the computed bond distances for the SOS and triplet states **5c** fit better with the experimental values than those calculated for the SCS (Table 2). Both functionals predict all three compounds **5a−c** to have a singlet open-shell ground state (referenced as zero), which is also in agreement with SQUID magnetic susceptibility measurements (upon cooling a solid sample of **5c**^{Menth}, χT decreases; see section S6 in Supporting Information). Interestingly, while in the case of **5a**^{Menth}, the cumulene (SCS) is only slightly higher in energy than the SOS (1.3−3.8 kcal/mol); this gap rises significantly in the case of **5b**^{Menth} (6.5−10 kcal/mol) and **5c**^{Menth} (13.0−16.7 kcal/mol). Concomitantly, the triplet state significantly drops in energy below the cumulene, thereby reducing the SOS-triplet gap from 4.0 to 4.2 kcal/mol (**5b**^{Menth}) to 1.3 kcal/mol (**5c**^{Menth}) (Figure 10).

DOI: 10.1021/jacs.7b11183
J. Am. Chem. Soc. 2018, 140, 2546−2554

Table 2. Comparison of Experimental and Calculated Bond Distances for 5c^{Menth}

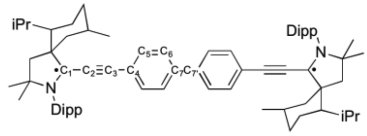

	N–C$_1$	C$_1$–C$_2$	C$_2$–C$_3$	C$_3$–C$_4$	C$_7$–C$_{7'}$	torsion angle (C$_7$–C$_{7'}$)
exp. *E*-isomer[a]	1.361(5)	1.368(5)	1.220(5)	1.386(5)	1.442(5)	1.9(6)
exp. *Z*-isomer[a]	1.356(5)	1.361(6)	1.221(6)	1.393(6)	1.439(5)	3.4(6)
SCS[b]	1.376	1.343	1.251	1.353	1.401	0.1
	1.369	1.347	1.252	1.357	1.405	6.1
SOS[b]	1.386	1.368	1.232	1.405	1.473	31
	1.378	1.370	1.235	1.404	1.471	32
triplet[b]	1.387	1.371	1.230	1.411	1.48	36
	1.379	1.373	1.233	1.410	1.479	36

[a]X-ray diffraction at 100 K; bond distances as average of left and right side of the molecule. [b]Calculated at the (U)/RCAM-B3LYP/6-31G** (top) and (U)/RM05-2X/6-31G** (bottom) level of theory for the *E*-isomer.

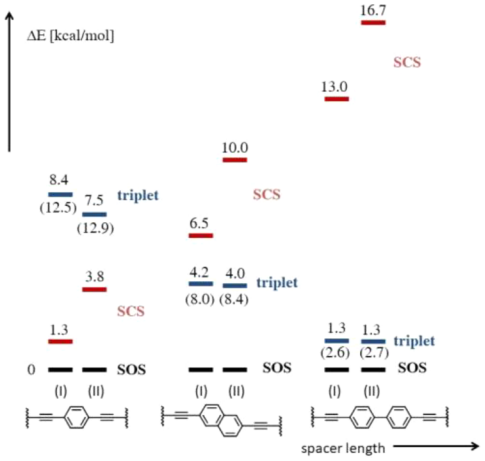

Figure 10. Comparison of electronic states of **5a–c** at (I) (U)M05-2X/6-31G** and (II) (U)CAM-B3LYP/6-31G** level of theory (in brackets with Yamaguchi spin-contamination correction).

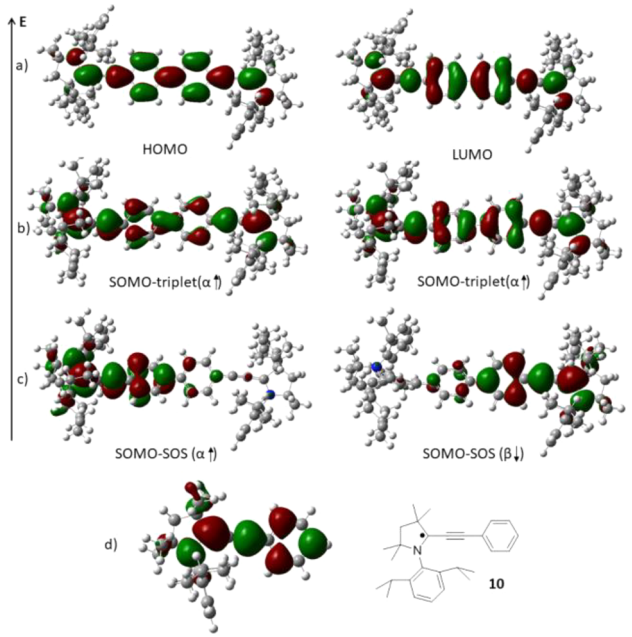

Figure 11. Molecular orbitals of the singlet closed-shell state (a), triplet state (b), and singlet open-shell state (c) of **5c** and SOMO of the monoradical **10** (d) at the R/(U)M05-2X/6-31G** level of theory.

Furthermore, the calculated values of the spin-operators <S^2> in the broken-symmetry approach are very close to 1, which indicates a very strong biradical character for both **5b** and **5c**. The frontier molecular orbitals of **5c** in its ground state (SOS), at the BS-UM05-2X/6-31G** level, show the singly occupied molecular orbital (SOMO) contribution over the individual sites with small overlap onto the other site, therefore resembling the SOMO of the monomeric radical **10** (Figure 11). We also explored the electronic structure of **5c** by CASSCF (see Supporting Information). The instability of the SCS state with increasing spacer length seems to be overestimated by DFT methods. The CASSCF calculations suggest a singlet ground state with strong multireference character and a very small singlet–triplet gap of 5.2 kcal mol^{-1}. The biradical character of the molecule should be high with a population of the LUMO of >0.6 electrons (biradical index = 0.6). Accordingly, both DFT and CASSCF predict a more pronounced biradical nature for **5c** than for **5a**.

SUMMARY

In summary, we have developed a modular approach for the synthesis of organic Kekulé diradicaloids in which the key step is based on the activation of terminal alkynes with CAACs. This synthetic route readily allows for the installation of spacers, featuring different degrees of aromaticity and length, and gives the possibility of generating unsymmetrical compounds with two different CAACs. This approach should also be applicable to other stable carbenes, and this is under current investigation. The Kekulé diradicaloids are stable at room temperature both in solution and in the solid state, which allowed for X-ray diffraction studies. These compounds, which are highly sensitive to oxygen, represent the first purely organic diradicaloids derived from iminium salts. While all Kekulé molecules reported here feature a singlet ground state, the spacer can modulate the biradical character and singlet–triplet gap. Interestingly, the diradicaloid featuring the longest spacer (ca. 15 Å between the CAAC moieties) exhibits properties similar to a comparable monoradical for which steric protection of the alkyne moiety is necessary to suppress decomposition pathways. We are currently investigating the use of the

DOI: 10.1021/jacs.7b11183
J. Am. Chem. Soc. 2018, 140, 2546–2554

synthetic strategy discussed here to prepare non-Kekulé di- and polyradicals.

■ ASSOCIATED CONTENT

Supporting Information

The Supporting Information is available free of charge on the ACS Publications website at DOI: 10.1021/jacs.7b11183.

Experimental procedures for the synthesis of each compound, along with the corresponding NMR, EPR, UV−vis/NIR spectra, and computational data (PDF)
CIF files for **4a**, **5a**, and **5c** (ZIP)

■ AUTHOR INFORMATION

Corresponding Author

*guybertrand@ucsd.edu

ORCID

Mohand Melaimi: 0000-0003-3553-1381
Dominik Munz: 0000-0003-3412-651X
Guy Bertrand: 0000-0003-2623-2363

Notes

The authors declare no competing financial interest.

■ ACKNOWLEDGMENTS

Thanks are due to the NSF (CHE-1661518) for financial support of this work and to the Alexander von Humboldt foundation for a Feodor-Lynen scholarship (M.M.H.). We are grateful to the Keck Foundation for funding the KeckII computer center, and we thank A. L. Rheingold, M. Gembicky, and C. E. Moore (X-ray diffraction), M. Tauber (EPR), and J. Hilgar and J. Rinehart for SQUID measurements.

■ REFERENCES

(1) For reviews on diradicals, see: (a) Salem, L.; Rowland, C. *Angew. Chem.* **1972**, *84*, 86. (b) Breher, F. *Coord. Chem. Rev.* **2007**, *251*, 1007. (c) Abe, M.; Ye, J.; Mishima, M. *Chem. Soc. Rev.* **2012**, *41*, 3808. (d) Abe, M. *Chem. Rev.* **2013**, *113*, 7011.

(2) Gomberg, M. *J. Am. Chem. Soc.* **1900**, *22*, 757.

(3) Tschitschibabin, A. E. *Ber. Dtsch. Chem. Ges.* **1907**, *40*, 1810.

(4) For a discussion about Tschitschibabin biradical, see for example: Ravat, P.; Baumgarten, M. *Phys. Chem. Chem. Phys.* **2015**, *17*, 983.

(5) For an overview, see for example: (a) Zeng, Z.; Shi, X.; Chi, C.; López Navarrete, J. T.; Casado, J.; Wu, J. *Chem. Soc. Rev.* **2015**, *44*, 6578. (b) Casado, J. *Top. Curr. Chem.* **2017**, *375*, 73. (c) Shi, X.; Chi, C. *Top. Curr. Chem.* **2017**, *375*, 68.

(6) (a) Montgomery, L. K.; Huffman, J. C.; Jurczak, E. A.; Grendze, M. P. *J. Am. Chem. Soc.* **1986**, *108*, 6004. (b) Zeng, Z.; Sung, Y. M.; Bao, N.; Tan, D.; Lee, R.; Zafra, J. L.; Lee, B. S.; Ishida, M.; Ding, J.; López Navarrete, J. T.; Li, Y.; Zeng, W.; Kim, D.; Huang, K.-W.; Webster, R. D.; Casado, J.; Wu, J. *J. Am. Chem. Soc.* **2012**, *134*, 14513.

(7) Thiele, J.; Balhorn, H. *Ber. Dtsch. Chem. Ges.* **1904**, *37*, 1463.

(8) (a) Su, Y.; Wang, X.; Zheng, X.; Zhang, Z.; Song, Y.; Sui, Y.; Li, Y.; Wang, X. *Angew. Chem., Int. Ed.* **2014**, *53*, 2857. (b) Su, Y.; Wang, X.; Wang, L.; Zhang, Z.; Wang, X.; Song, Y.; Power, P. P. *Chem. Sci.* **2016**, *7*, 6514. (c) Zheng, S.; Barlow, S.; Risko, C.; Kinnibrugh, T. L.; Khrustalev, V. N.; Jones, S. C.; Antipin, M. Y.; Tucker, N. M.; Timofeeva, T. V.; Coropceanu, V.; Brédas, J.-L.; Marder, S. R. *J. Am. Chem. Soc.* **2006**, *128*, 1812. (d) Ito, A.; Urabe, M.; Tanaka, K. *Angew. Chem., Int. Ed.* **2003**, *42*, 921. (e) Li, T.; Tan, G.; Shao, D.; Li, J.; Zhang, Z.; Song, Y.; Sui, Y.; Chen, S.; Fang, Y.; Wang, X. *J. Am. Chem. Soc.* **2016**, *138*, 10092. (f) Tan, G.; Wang, X. *Acc. Chem. Res.* **2017**, *50*, 1997.

(9) (a) Sun, Z.; Zeng, Z.; Wu, J. *Acc. Chem. Res.* **2014**, *47*, 2582. (b) Huang, R.; Phan, H.; Herng, T. S.; Hu, P.; Zeng, W.; Dong, S.-Q.; Das, S.; Shen, Y.; Ding, J.; Casanova, D.; Wu, J. *J. Am. Chem. Soc.* **2016**, *138*, 10323. (c) Hsieh, Y.-C.; Fang, H.-Y.; Chen, Y.-T.; Yang, R.; Yang, C.; Chou, P.-T.; Kuo, M.-Y.; Wu, Y. T. *Angew. Chem.* **2015**, *127*, 3112.

(10) See for examples: (a) Ji, L.; Edkins, R. M.; Lorbach, A.; Krummenacher, I.; Brückner, C.; Eichhorn, A.; Braunschweig, H.; Engels, B.; Low, P. J.; Marder, T. B. *J. Am. Chem. Soc.* **2015**, *137*, 6750. (b) Niecke, E.; Fuchs, A.; Baumeister, F.; Nieger, M.; Schoeller, W. W. *Angew. Chem., Int. Ed. Engl.* **1995**, *34*, 555. (c) Cui, C.; Brynda, M.; Olmstead, M. M.; Power, P. P. *J. Am. Chem. Soc.* **2004**, *126*, 6510. (d) Cox, H.; Hitchcock, P. B.; Lappert, M. F.; Pierssens, L. J.-M. *Angew. Chem., Int. Ed.* **2004**, *43*, 4500. (e) Bourg, J.-B.; Rodriguez, A.; Scheschkewitz, D.; Gornitzka, H.; Bourissou, D.; Bertrand, G. *Angew. Chem., Int. Ed.* **2007**, *46*, 5741. (f) Takeuchi, K.; Ichinohe, M.; Sekiguchi, A. *J. Am. Chem. Soc.* **2011**, *133*, 12478. (g) Nozawa, T.; Nagata, M.; Ichinohe, M.; Sekiguchi, A. *J. Am. Chem. Soc.* **2011**, *133*, 5773. (h) Power, P. P. *Chem. Rev.* **2003**, *103*, 789. (i) Lee, V. Y.; Sekiguchi, A. *Acc. Chem. Res.* **2007**, *40*, 410. (j) Grützmacher, H.; Breher, F. *Angew. Chem., Int. Ed.* **2002**, *41*, 4006. (k) Rajca, A.; Lu, K.; Rajca, S.; Ross, C. R., II *Chem. Commun.* **1999**, 1249. (l) Scheschkewitz, D.; Amii, H.; Gornitzka, H.; Schoeller, W. W.; Bourissou, D.; Bertrand, G. *Science* **2002**, *295*, 1880. (m) Scheschkewitz, D.; Amii, H.; Gornitzka, H.; Schoeller, W. W.; Bourissou, D.; Bertrand, G. *Angew. Chem., Int. Ed.* **2004**, *43*, 585.

(11) See for examples: (a) Ravat, P.; Ito, Y.; Gorelik, E.; Enkelmann, V.; Baumgarten, M. *Org. Lett.* **2013**, *15*, 4280. (b) Osiecki, J. H.; Ullman, E. F. *J. Am. Chem. Soc.* **1968**, *90*, 1078. (c) Osiecki, J. H.; Ullman, E. F. *J. Am. Chem. Soc.* **1968**, *90*, 1078. (d) Ravat, P.; Teki, Y.; Ito, Y.; Gorelik, E.; Baumgarten, M. *Chem. - Eur. J.* **2014**, *20*, 12041. (e) Train, C.; Norel, L.; Baumgarten, M. *Coord. Chem. Rev.* **2009**, *253*, 2342.

(12) (a) Rajca, A. *Chem. Rev.* **1994**, *94*, 871. (b) Morita, Y.; Suzuki, K.; Sato, S.; Takui, T. *Nat. Chem.* **2011**, *3*, 197. (c) Lambert, C. *Angew. Chem., Int. Ed.* **2011**, *50*, 1756. (d) Sun, Z.; Wu, J. *J. Mater. Chem.* **2012**, *22*, 4151. (e) Sun, Z.; Ye, Q.; Chi, C.; Wu, J. *Chem. Soc. Rev.* **2012**, *41*, 7857. (f) Kamada, K.; Ohta, K.; Kubo, T.; Shimizu, A.; Morita, Y.; Nakasuji, K.; Kishi, R.; Ohta, S.; Furukawa, S.; Takahashi, H.; Nakano, M. *Angew. Chem., Int. Ed.* **2007**, *46*, 3544.

(13) For the synthesis of CAACs, see: (a) Lavallo, V.; Canac, Y.; Präsang, C.; Donnadieu, B.; Bertrand, G. *Angew. Chem., Int. Ed.* **2005**, *44*, 5705. (b) Jazzar, R.; Dewhurst, R. D.; Bourg, J. B.; Donnadieu, B.; Canac, Y.; Bertrand, G. *Angew. Chem., Int. Ed.* **2007**, *46*, 2899. (c) Jazzar, R.; Bourg, J. B.; Dewhurst, R. D.; Donnadieu, B.; Bertrand, G. *J. Org. Chem.* **2007**, *72*, 3492. (d) Zeng, X.; Frey, G. D.; Kinjo, R.; Donnadieu, B.; Bertrand, G. *J. Am. Chem. Soc.* **2009**, *131*, 8690. (e) Tomás-Mendivil, E.; Hansmann, M. M.; Weinstein, C. M.; Jazzar, R.; Melaimi, M.; Bertrand, G. *J. Am. Chem. Soc.* **2017**, *139*, 7753.

(14) For reviews, see: (a) Melaimi, M.; Jazzar, R.; Soleilhavoup, M.; Bertrand, G. *Angew. Chem., Int. Ed.* **2017**, *56*, 10046. (b) Paul, U. S. D.; Radius, U. *Eur. J. Inorg. Chem.* **2017**, *2017*, 3362. (c) Soleilhavoup, M.; Bertrand, G. *Acc. Chem. Res.* **2015**, *48*, 256. (d) Melaimi, M.; Soleilhavoup, M.; Bertrand, G. *Angew. Chem., Int. Ed.* **2010**, *49*, 8810. (e) Droege, T.; Glorius, F. *Angew. Chem., Int. Ed.* **2010**, *49*, 6940. (f) Martin, D.; Melaimi, M.; Soleilhavoup, M.; Bertrand, G. *Organometallics* **2011**, *30*, 5304. (g) Hahn, F. E.; Jahnke, M. C. *Angew. Chem., Int. Ed.* **2008**, *47*, 3122.

(15) (a) Mahoney, J. K.; Martin, D.; Moore, C. E.; Rheingold, A. L.; Bertrand, G. *J. Am. Chem. Soc.* **2013**, *135*, 18766. (b) Mahoney, J. K.; Martin, D.; Thomas, F.; Moore, C. E.; Rheingold, A. L.; Bertrand, G. *J. Am. Chem. Soc.* **2015**, *137*, 7519. (c) Mahoney, J. K.; Jazzar, R.; Royal, G.; Martin, D.; Bertrand, G. *Chem. - Eur. J.* **2017**, *23*, 6206. (d) Styra, S.; Melaimi, M.; Moore, C. E.; Rheingold, A. L.; Augenstein, T.; Breher, F.; Bertrand, G. *Chem. - Eur. J.* **2015**, *21*, 8441. (e) Hansmann, M. M.; Melaimi, M.; Bertrand, G. *J. Am. Chem. Soc.* **2018**, 2206.

(16) See for examples: (a) Weinberger, D. S.; Melaimi, M.; Moore, C. E.; Rheingold, A. L.; Frenking, G.; Jerabek, P.; Bertrand, G. *Angew. Chem., Int. Ed.* **2013**, *52*, 8964. (b) Singh, A. P.; Samuel, P. P.; Roesky, H. W.; Schwarzer, M. C.; Frenking, G.; Sidhu, N. S.; Dittrich, B. *J. Am. Chem. Soc.* **2013**, *135*, 7324. (c) Mondal, K. C.; Samuel, P. P.; Roesky, H. W.; Carl, E.; Herbst-Irmer, R.; Stalke, D.; Schwederski, B.; Kaim, W.; Ungur, L.; Chibotaru, L. F.; Hermann, M.; Frenking, G. *J. Am.*

DOI: 10.1021/jacs.7b11183
J. Am. Chem. Soc. 2018, 140, 2546−2554

Chem. Soc. **2014**, *136*, 1770. (d) Ung, G.; Rittle, J.; Soleilhavoup, M.; Bertrand, G.; Peters, J. C. *Angew. Chem., Int. Ed.* **2014**, *53*, 8427. (e) Kinjo, R.; Donnadieu, B.; Bertrand, G. *Angew. Chem., Int. Ed.* **2010**, *49*, 5930. (f) Back, O.; Celik, M. A.; Frenking, G.; Melaimi, M.; Donnadieu, B.; Bertrand, G. *J. Am. Chem. Soc.* **2010**, *132*, 10262. (g) Kinjo, R.; Donnadieu, B.; Celik, M. A.; Frenking, G.; Bertrand, G. *Science* **2011**, *333*, 610. (h) Mondal, K. C.; Roesky, H. W.; Schwarzer, M. C.; Frenking, G.; Tkach, I.; Wolf, H.; Kratzert, D.; Herbst-Irmer, R.; Niepötter, B.; Stalke, D. *Angew. Chem., Int. Ed.* **2013**, *52*, 1801. (i) Abraham, M. Y.; Wang, Y.; Xie, Y.; Gilliard, R. J., Jr.; Wei, P.; Vaccaro, B. J.; Johnson, M. K.; Schaefer, H. F., III; Schleyer, P. v. R.; Robinson, G. H. *J. Am. Chem. Soc.* **2013**, *135*, 2486. (j) Kretschmer, R.; Ruiz, D. A.; Moore, C. E.; Rheingold, A. L.; Bertrand, G. *Angew. Chem., Int. Ed.* **2014**, *53*, 8176. (k) Martin, D.; Moore, C. E.; Rheingold, A. L.; Bertrand, G. *Angew. Chem., Int. Ed.* **2013**, *52*, 7014. (l) Roy, S.; Stückl, A. C.; Demeshko, S.; Dittrich, B.; Meyer, J.; Maity, B.; Koley, D.; Schwederski, B.; Kaim, W.; Roesky, H. W. *J. Am. Chem. Soc.* **2015**, *137*, 4670.

(17) For reviews on the stabilization of radicals by carbenes, see: (a) Martin, C. D.; Soleilhavoup, M.; Bertrand, G. *Chem. Sci.* **2013**, *4*, 3020. (b) Chandra Mondal, K.; Roy, S.; Roesky, H. W. *Chem. Soc. Rev.* **2016**, *45*, 1080.

(18) (a) Singh, A. P.; Samuel, P. P.; Roesky, H. W.; Schwarzer, M. C.; Frenking, G.; Sidhu, N. S.; Dittrich, B. *J. Am. Chem. Soc.* **2013**, *135*, 7324. (b) Samuel, P. P.; Mondal, K. C.; Roesky, H. W.; Hermann, M.; Frenking, G.; Demeshko, S.; Meyer, F.; Stückl, A. C.; Christian, J. H.; Dalal, N. S.; Ungur, L.; Chibotaru, L. F.; Pröpper, K.; Meents, A.; Dittrich, B. *Angew. Chem., Int. Ed.* **2013**, *52*, 11817.

(19) Mondal, K. C.; Roesky, H. W.; Schwarzer, M. C.; Frenking, G.; Tkach, I.; Wolf, H.; Kratzert, D.; Herbst-Irmer, R.; Niepötter, B.; Stalke, D. *Angew. Chem., Int. Ed.* **2013**, *52*, 1801.

(20) (a) Li, Y.; Mondal, K. C.; Samuel, P. P.; Zhu, H.; Orben, C. M.; Panneerselvam, S.; Dittrich, B.; Schwederski, B.; Kaim, W.; Mondal, T.; Koley, D.; Roesky, H. W. *Angew. Chem., Int. Ed.* **2014**, *53*, 4168. (b) Jin, L.; Melaimi, M.; Liu, L.; Bertrand, G. *Org. Chem. Front.* **2014**, *1*, 351.

(21) For carbene-stabilized C_2, see for example: Georgiou, D. C.; Stringer, B. D.; Hogan, C. F.; Barnard, P. J.; Wilson, D. J. D.; Holzmann, N.; Frenking, G.; Dutton, J. L. *Chem. - Eur. J.* **2015**, *21*, 3377.

(22) (a) Turner, Z. R. *Chem. - Eur. J.* **2016**, *22*, 11461. (b) Jin, L.; Melaimi, M.; Kostenko, A.; Karni, M.; Apeloig, Y.; Moore, C. E.; Rheingold, A. L.; Bertrand, G. *Chem. Sci.* **2016**, *7*, 150. (c) Hansmann, M. M.; Melaimi, M.; Bertrand, G. *J. Am. Chem. Soc.* **2017**, *139*, 15620.

(23) During the revision process of this Article, the synthesis and characterization of a bis(NHC) analogue of **5a**, which features a quinoidal character was reported: Barry, B. M.; Soper, R. G.; Hurmalainen, J.; Mansikkamäki, A.; Robertson, K. N.; McClennan, W. L.; Veinot, A. J.; Roemmele, T. L.; Werner-Zwanziger, U.; Boeré, R. T.; Tuononen, H. M.; Clyburne, J. A. C.; Masuda, J. D. *Angew. Chem., Int. Ed.* **2018**, *57*, 749.

(24) Mondal, K. C.; Samuel, P. P.; Roesky, H. W.; Niepötter, B.; Herbst-Irmer, R.; Stalke, D.; Ehret, F.; Kaim, W.; Maity, B.; Koley, D. *Chem. - Eur. J.* **2014**, *20*, 9240.

(25) See for example: Kamada, K.; Fuku-en, S.; Minamide, S.; Ohta, K.; Kishi, R.; Nakano, M.; Matsuzaki, H.; Okamoto, H.; Higashikawa, H.; Inoue, K.; Kojima, S.; Yamamoto, Y. *J. Am. Chem. Soc.* **2013**, *135*, 232.

(26) For examples, see: Zafra, J. L.; González Cano, R. C.; Ruiz Delgado, M. C.; Sun, Z.; Li, Y.; López Navarrete, J. T.; Wu, J.; Casado, J. *J. Chem. Phys.* **2014**, *140*, 054706.

(27) (a) Noodleman, L. *J. Chem. Phys.* **1981**, *74*, 5737. (b) Noodleman, L.; Baerends, E. J. *J. Am. Chem. Soc.* **1984**, *106*, 2316. (c) Yamaguchi, K.; Takahara, Y.; Fueno, T.; Nasu, K. *Jpn. J. Appl. Phys.* **1987**, *26*, L1362. (d) Yamaguchi, K.; Jensen, F.; Dorigo, A.; Houk, K. N. *Chem. Phys. Lett.* **1988**, *149*, 537.

(28) Charbonneau, G.-P.; Delugeard, Y. *Acta Crystallogr., Sect. B: Struct. Crystallogr. Cryst. Chem.* **1977**, *33*, 1586.

(29) Cailleau, H.; Baudour, J. L.; Zeyen, C. M. E. *Acta Crystallogr., Sect. B: Struct. Crystallogr. Cryst. Chem.* **1979**, *35*, 426.

(30) Porter, W. W., III; Vaid, T. P.; Rheingold, A. L. *J. Am. Chem. Soc.* **2005**, *127*, 16559.

DOI: 10.1021/jacs.7b11183
J. Am. Chem. Soc. 2018, 140, 2546−2554